

# The dependence of dark halo clustering on the formation epoch and the concentration parameter

Y. P. Jing

*Shanghai Astronomical Observatory, Nandan Road 80, Shanghai, 200030, China*

Yasushi Suto

*Department of Physics and Research Center for the Early Universe (RESCEU)  
School of Science, University of Tokyo, Tokyo 113-0033, Japan*

and

H.J. Mo

*Department of Astronomy, University of Massachusetts, Amherst MA 01003-9305*

*e-mail: ypjing@shao.ac.cn, suto@phys.s.u-tokyo.ac.jp, hjmo@nova.astro.umass.edu*

## ABSTRACT

We examine the age-dependence of dark matter halo clustering in an unprecedented accuracy using a set of 7 high-resolution cosmological simulations each with  $N = 1024^3$  particles. We measure the bias parameters for halos over a large mass range using the cross-power-spectrum method that can effectively suppress the random noise even in the sparse sampling of the most massive halos. This enables us to find, for the first time, that younger halos are more strongly clustered than older ones for halo masses  $M > 10M_*$ , where  $M_*$  is the characteristic nonlinear mass scale. For  $M < M_*$ , our results confirm the previous finding of Gao et al. that older halos are clustered more strongly than the younger ones. We also study the halo bias as a function of halo concentration, and find that the concentration dependence is weaker than the age dependence for  $M < M_*$ , but stronger for  $M \gtrsim 50M_*$ . The accurate and robust measurement of the age dependences of halo bias points to a limitation of the simple excursion set theory which predicts that the formation and structure of a halo of given mass is independent of its environment.

*Subject headings:* gravitational lensing—dark matter— cosmology: theory— galaxies: formation

## 1. Introduction

The formation of dark matter halos plays a central role in the studies of galaxy formation as well as of the large-scale structure of the universe. A widely used analytical theory for the formation of halos is the extended Press-Schechter (PS thereafter) formalism (Bond et al. 1991; Bower 1991), which can be used to model the mass function of dark halos (Press & Schechter 1974), the bias parameter as a function of halo mass (Mo & White 1996, hereafter MW96), as well as the formation histories of dark halos (Lacey & Cole 1993, 1994). In the simplest excursion-set model of Bond et al. (1991), the physical properties of dark halos are expected to depend only on halo mass, but not on large-scale environments. However, it has been known for almost a decade that neither the PS mass function nor the MW96 bias model matches well  $N$ -body results for halo masses  $M < M_*$ , where  $M_*$  is defined such that the rms linear density fluctuation within a sphere of mass  $M_*$  is  $\delta_c = 1.68$  (Jing 1998; Lee & Shandarin 1998; Sheth & Lemson 1999; Porciani et al. 1999; Jing 1999; Sheth & Tormen 1999). Sheth et al. (2001) proposed an ellipsoid collapse model to replace the spherical collapse model in the PS theory, and found a better agreement between the theory and  $N$ -body simulations in both the mass function and the bias function. Earlier investigations with cosmological  $N$ -body simulations did not find any strong environmental dependence of halo properties, such as the spin parameter, concentration and formation time (Lemson & Kauffmann 1999; Percival et al. 2003). However, the poor resolutions and small dynamical ranges covered in these simulations make it difficult to detect any signals that are relatively weak or outside the dynamical range, and so a significant age-dependence of halo clustering cannot be ruled out. Note also that there were earlier attempts to develop empirical models for the age-dependence of halo clustering (Taruya & Suto 2000; Hamana et al. 2001; Yoshikawa et al. 2001).

With the use of a very large  $N$ -body simulation, Gao et al. (2005) recently demonstrated convincingly that the clustering strength of dark halos does depend on halo formation time. In particular, they found that this dependence is strong only for halos with  $M \ll M_*$  and becomes very weak for  $M > M_*$ . This also explains why Percival et al. (2003) could not detect an age dependence, because they focused on halos with  $M > M_*$  at high redshifts. Wang et al. (2006) have examined the physical process that may be responsible for the age dependence of halo clustering. They found that halos embedded in dense environments accrete mass less efficiently than the spherical collapse model predicts, because the matter to be accreted is ‘heated’ by the large-scale structure (like the pancake heating considered in, e.g., Mo et al. 2005; Lee 2006). This explains why the old population of small halos has a higher bias than the young population of the same mass. It also qualitatively explains why the PS mass function and bias functions deviate from  $N$ -body simulations at small masses.

It is well known that the concentration parameter of halos at a given mass,  $c(M)$ , has a broad log-normal distribution, and is correlated with the halo formation epoch  $z_{\text{form}}$  in such a way that halos of earlier formation have a higher concentration (Jing 2000; Bullock et al. 2001; Jing & Suto 2002; Wechsler et al. 2002; Zhao et al. 2003a,b). Therefore the age dependence of halo bias should yield a concentration dependence of halo bias. Such dependence is indeed observed in recent  $N$ -body simulations. Wechsler et al. (2006) found that, for masses  $M < M_*$ , halos with higher concentrations are more strongly clustered, as expected from the age dependence and the correlation between the age and concentration of dark halos. More interestingly, Wechsler et al. (2006) found reversed concentration dependence for  $M > M_*$ , in the sense that halos with higher concentrations are actually less biased. This result was not seen by Gao et al. (2005) who explored the age dependence only for  $M \leq 10M_*$ . More recently, Wetzel et al. (2006) examined both the age dependence and concentration dependence of halo clustering for massive halos. While they found concentration dependence similar to that found by Wechsler et al. (2006), they did not detect any significant dependence on formation epoch. Note, however, that Wechsler et al. (2006) used halos identified at different redshifts to increase the dynamical range probed by their simulations, while both Gao et al. (2005) and Wetzel et al. (2006) used halos identified at the same time. It is unclear how to make a detailed comparison between the different results.

The environmental dependence of halo formation and structure has important implications not only for improving the PS theory but also for improving semi-analytical models of galaxy formation based on PS merger trees and current halo occupation distribution (HOD) models. In this *Letter*, we use a large set of cosmological simulations, each with  $1024^3$  particles, to investigate in detail the concentration and formation epoch dependence of halo clustering.

## 2. Simulations

The model considered here is a canonical spatially-flat Cold Dark Matter (CDM) model with the density parameter  $\Omega_m = 0.268$ , the cosmological constant  $\Omega_\Lambda = 0.732$ , the Hubble constant  $h = 0.71$ , and the baryon density parameter  $\Omega_b = 0.045$ . The primordial density field is assumed to be Gaussian with a scale-invariant power spectrum  $\propto k$ . For the linear spectrum, we adopt the fitting transfer function of Eisenstein & Hu (1998), and the normalization is set by  $\sigma_8 = 0.85$ , where  $\sigma_8$  is the present linear RMS density fluctuation within a sphere of radius  $8 h^{-1}\text{Mpc}$ .

We use an upgraded version of the Particle-Particle-Particle-Mesh (P<sup>3</sup>M) code of Jing & Suto (1998, 2002) to simulate structure formation in the universe. The code has now incorporated

the multiple level P<sup>3</sup>M gravity solver for high density regions (Jing & Suto 2000). In order to have a large mass resolution range, we run a total of 7 simulations with 1024<sup>3</sup> particles in different simulation boxes (Table 1). The simulations were run on an SGI Altix 350 with 16 processors with OPENMP parallelization in Shanghai Astronomical Observatory. We have 4 realizations with boxsize 1800  $h^{-1}$ Mpc in order to reliably measure the bias of the most massive halos, which is the focus of the present *Letter*.

Dark matter halos are identified using the standard Friends-of-Friends algorithm with a linking length  $b$  equal to 0.2 times the mean particle separation. Unbound particles (with positive binding energy) are excluded. We use halos containing 100 particles or more, and our analysis covers halos with masses ranging from  $2 \times 10^{11} h^{-1}M_{\odot}$  to  $10^{15} h^{-1}M_{\odot}$ .

### 3. Clustering of dark matter halos

#### 3.1. Cross power spectrum and the halo bias

Once the number density field of dark matter halos,  $n_h(\mathbf{r})$ , and the density field of dark matter  $\rho_m(\mathbf{r})$ , are given, the conventional way to estimate the halo bias factor  $b$  is to use the definition,  $b \equiv (\xi_{hh}(r)/\xi_{mm}(r))^{1/2}$ , where  $\xi_{hh}(r)$  is the two-point correlation function of dark halos, and  $\xi_{mm}(r)$  that of dark matter. Here we adopt a slightly different approach by using the cross power spectrum of Jing (1999). We first Fourier transform both  $n_h(\mathbf{r})$  and  $\rho_m(\mathbf{r})$  into  $n_h(\mathbf{k})$  and  $\rho_m(\mathbf{k})$ , and then measure the bias factor through

$$b \equiv \frac{P_{hm}(k)}{P_{mm}(k)} = \frac{\bar{\rho}_m}{\bar{n}_h} \frac{\langle n_h(\mathbf{k})\rho_m(\mathbf{k}) \rangle}{\langle \rho_m(\mathbf{k})\rho_m(\mathbf{k}) \rangle}. \quad (1)$$

As shown by Jing (1999), this method suppresses Poisson noise due to a limited number of dark halos more effectively than the correlation method, because the number of dark particles is in general much larger than that of dark halos. This is particularly important for the present study, as we need to accurately determine the bias for massive halos whose number density is low. We have estimated the bias factors for the four realizations of the 1800  $h^{-1}$ Mpc box simulations, using both the correlation method and the cross power spectrum method. The average values of the bias over the four realizations obtained with the two methods are consistent, but the scatter with the correlation method is about a factor of 2 larger than that with the cross power spectrum. The cross power spectrum method is therefore preferred.

Errors on  $b(k)$  are estimated following Jing (1999): ten random samples are generated for each simulated halo sample, and the scatter of  $b(k)$  among them is used as the error in  $b(k)$  for the real sample. We have compared the error so obtained with that estimated from

the scatter among the 4 realizations of the  $1800 h^{-1}\text{Mpc}$  box simulation. The errors given by the two methods are comparable.

### 3.2. Dependence on the halo formation epoch

Our analysis focuses on the halo populations at the present time,  $z = 0$ . Halos are divided into mass bins (specified by  $[m_1, m_2]$  with  $m_2 = 2m_1$ ) according to their masses. For each mass bin, we sort the halos into 5 populations according to formation redshift,  $z_f$ , which is defined as the redshift at which the mass of the most massive progenitor of a halo is equal to half of its mass. Although analysis was carried out for all the five populations, here we present the results only for the 20% youngest halos with the smallest  $z_f$  and for the 20% oldest ones with the largest  $z_f$ . In what follows, these two populations are simply referred to as the young and the old populations, respectively. To ensure that the bias obtained here is in the linear regime, we only consider Fourier modes with  $k < k_{max}$ , where  $k_{max} = 0.09 h\text{Mpc}^{-1}$  is a wavenumber at which the variance  $\Delta^2(k_{max}) \equiv k_{max}^3 P_{mm}(k_{max})/2\pi^2 = 0.25$ . Figure 1 plots examples of the bias factor for massive halos with  $M = 35M_*$  and  $M = 134M_*$ , where  $M_* = 5 \times 10^{12} h^{-1} M_\odot$ , in the  $1800 h^{-1}\text{Mpc}$  box simulations. The top-left panel shows the results for the young population, while the top-right panel shows the same measurement for the old population. The results clearly show that the bias factors are nearly scale independent in the linear regime. The solid line in each panel is the mean value obtained by a least square fit to the data points at  $k < k_{max}$ . The bias factor for the young population is about 10% higher than that for old population.

We present the mean bias factor  $b(M)$  as a function of mass obtained from different simulations in the top panel of Figure 2. For a given halo mass, the measurement of  $b(M)$  is more accurate in a simulation of a larger volume. Therefore we plot the data points for each simulation only up to a halo mass which corresponds to 100 particles in the next larger simulation, except for the  $1800 h^{-1}\text{Mpc}$  box simulation, where we plot all the data points available. Note that the bias factors obtained from different simulations agree extremely well with each other, and so the set of simulations used here allows us to explore the age dependence of halo bias over four orders of magnitude in halo mass. For  $M < 3M_*$ , the old population (red symbols) is more strongly biased (has stronger clustering) than the young population (blue symbols), which is in a good quantitative agreement with the results obtained by Gao et al. (2005, cyan lines). With the Millennium Simulation with a boxsize of  $500 h^{-1}\text{Mpc}$ , Gao et al. (2005) was not able to explore accurately the age dependence of halo clustering for higher halo mass. Our results clearly show that the difference between the old and young populations decreases with increasing halo mass up to  $M \approx 10M_*$ , at which the

young population starts to surpass the old population in the bias factor. For  $M > 20M_*$ , the bias factor for the young population is about 10% higher than that of the old population, with weak dependence on halo mass. Although the difference in the bias factor between the old and young populations is small at the high mass end, it is detected at a high statistical confidence ( $\sim 10\sigma$ ).

### 3.3. Dependence on halo concentration

The concentration of each halo is obtained following the fitting method of Jing (2000). The density distribution within each halo is fitted with a NFW profile to obtain the scale radius  $r_s$ , and the concentration is defined as  $c = r_v/r_s$ , where  $r_v$  is the virial radius within which the mean density is 361 times the mean density of the universe. Here only halos with 320 particles or more are used, because the concentration may not be measured accurately for halos containing smaller number of particles (e.g. Wechsler et al. 2006).

The lower two panels of Figure 1 show the bias factor as a function of wavenumber for massive halos with  $M = 35M_*$  and  $M = 134M_*$ . Results for the least concentrated 20% are plotted in the lower left panel, while those for the most concentrated 20% are in the lower right panel. Here again, the bias factor is almost scale-independent. The amplitude of the bias factor for massive halos clearly depends on concentration, with halos with higher concentration less strongly biased. To see how the concentration-dependence changes with halo mass, we plot in the lower panel of Figure 2 the bias factor for the most concentrated 20% and the least concentrated 20% of the halos in each of the mass bins. Note that there is good agreement between simulations with different box sizes, suggesting that 320 particles may be sufficient to sample the concentration for the purpose of the present paper. Our results show clearly that the more concentrated halos have a larger bias for  $M < M_*$ , but the trend is reversed for  $M > M_*$ , in qualitative agreement with the results in Wechsler et al. (2006).

Comparing the results here with the dependence on the formation epoch (the upper panel), we see that the concentration dependence is weaker than the age dependence for  $M < M_*$ , but stronger for  $M \gg M_*$ . The difference in the bias factor between the most concentrated 20% and the least concentrated 20% is about 25% for  $M = 10M_* - 100M_*$ , larger than the 10% between the youngest 20% and oldest 20%. This may be why concentration dependence was but age dependence was not found for halos with  $M > M_*$  in previous investigations (Gao et al. 2005; Zhu et al. 2006; Wechsler et al. 2006; Wetzel et al. 2006). Our results also show that the concentration dependence reverses almost exactly at  $M = M_*$ , while the reversal of age dependence occurs at a much larger mass,  $M \approx 10M_*$ . Finally, the concentration dependence does not seem to become stronger with increasing mass for

$M > M_*$ . In fact, the difference in the bias factor between the most concentrated 20% and the least concentrated 20% is only about 10% at  $250M_*$ .

### 3.4. The effect of finite mass bins

So far we have used a finite mass bin  $[M_1, M_2]$  with  $M_2 = 2M_1$  to study the age and concentration dependence of the bias for halos of a given mass. Since more massive halos on average have younger ages and smaller concentration, and since the bias factor increases strongly with halo mass at the high mass end, the use of a finite mass bin to represent a given mass may artificially introduce age and concentration dependence. To check this effect, we repeat our analysis using narrower mass bins with  $M_2 = 1.2M_1$ . The results are plotted as the solid and dashed lines in Figure 2. The results are almost indistinguishable from those obtained with  $M_2 = 2M_1$ , demonstrating that the mass bins we used is sufficiently small.

## 4. Summary and Discussion

Our major findings in this paper can be summarized as follows:

- (i) The younger halo population is significantly less clustered than the old one for  $M < 10M_*$ ;
- (ii) For  $M > 10M_*$ , the age dependence is reversed, and the bias factor of the youngest 20% of the halos with a given mass is approximately 10% *higher* than that of the oldest 20% of the same mass;
- (iii) When the halos are divided into subsamples according to concentration parameter, the halo bias is larger (smaller) for halos with higher concentrations for  $M < M_*$  ( $M > M_*$ ).

The first result is a confirmation of the result of Gao et al. (2005) with the use of a much larger data set and a different clustering measure (our cross power spectrum versus their auto-correlation function). Our use of a large set of simulations in large boxes enables us to quantify, for the first time, the age dependence of halo bias for  $M > 10M_*$ . The weak age dependence for massive halos relative to low-mass halos ones may reflect the fact that these halos have a narrower distribution in formation time (see Fig.1 of Kitayama & Suto 1996b), but the opposite trend, although weak, is not easy to explain. The third result is qualitatively in agreement with Wechsler et al. (2006). However, their results are based on

halos identified at different times, while ours are based on halos identified at the same time as it should be. Our results also show that the concentration dependence is weaker than the age dependence for  $M < M_*$  but stronger for  $M \sim 50M_*$ . There is also indication that both the age and concentration dependence becomes weaker at the very massive end.

The difference in the age and concentration dependence implies that caution must be taken in comparing model predictions with observational results (e.g. Yang et al. 2006), since it is unclear whether the formation epoch, as defined by  $z_f$ , or concentration, or even some other properties of a halo is more important in determining the properties of the galaxies that form in it.

The dependence of halo bias on formation epoch and concentration implies that the simple excursion set theory of halo formation (Press & Schechter 1974; Bower 1991; Bond et al. 1991) is not accurate. As discussed in Wang et al. (2006), the problem with the simple excursion set theory is that spherical collapse model, which neglects large-scale tidal field, over-predicts the collapse of small halos ( $\ll M_*$ ) in high density environments. They argue, however, that this dynamical effect should be smaller for large halos ( $M \gg M_*$ ). It is possible that the large-scale tidal field also plays a role in the formation of massive halos. But instead of truncating mass accretion, as is for the case of low-mass halos, the large-scale tidal field may delay the accretion, enhancing the accretion at later times. This possibility should be checked further by examining in detail the accretion histories and environments of massive halos in simulations.

The extended PS theory (Lacey & Cole 1993, 1994; Sasaki 1994; Kitayama & Suto 1996a) has been implemented in a variety of cosmological studies with clusters of galaxies (Kitayama & Suto 1996b, 1997; Taruya & Suto 2000; Hamana et al. 2001). The present results for massive halos point to a limitation of the theory in such applications, and indeed should prompt the exploration of an improved theoretical framework in the future.

We thank Liang Gao for providing the data plotted in Figure 2. YPJ is supported by NSFC(10373012, 10533030) and by Shanghai Key Projects in Basic Research (04jc14079, 05xd14019). The research of YS is partly supported by Grant-in-Aid for Scientific Research of Japan Society for Promotion of Science (No.14102004, 16340053). HJM would like to acknowledge the support of NSF AST-0607535. The visit of HJM to Shanghai Observatory was supported by the CAS scholar program.



## REFERENCES

- Bond J.R., Cole S., Efstathiou G. & Kaiser N., 1991, *ApJ*, 379, 440
- Bower, R. G. 1991, *MNRAS*, 248, 332
- Bullock, J. S., Kolatt, T. S., Sigad, Y., Somerville, R. S., Kravtsov, A. V., Klypin, A. A., Primack, J. R., & Dekel, A. 2001, *MNRAS*, 321, 559
- Eisenstein, D. J., & Hu, W. 1998, *ApJ*, 496, 605
- Gao L., Springel V. & White S.D.M., 2005, *MNRAS*, 363, L66
- Hamana, T., Yoshida, N., Suto, Y., & Evrard, A. E. 2001, *ApJ*, 561, L143
- Jing, Y. P. 1998, *ApJ*, 503, L9
- Jing, Y. P. 1999, *ApJ*, 515, L45
- Jing, Y. P. 2000, *ApJ*, 535, 30
- Jing, Y. P., & Suto, Y. 1998, *ApJ*, 494, L5
- Jing, Y. P., & Suto, Y. 2000, *ApJ*, 529, L69
- Jing, Y. P., & Suto, Y. 2002, *ApJ*, 574, 538
- Kitayama, T., & Suto, Y. 1996a, *MNRAS*, 280, 638
- Kitayama, T., & Suto, Y. 1996b, *ApJ*, 469, 480
- Kitayama, T., & Suto, Y. 1997, *ApJ*, 490, 557
- Lacey, C., & Cole, S. 1993, *MNRAS*, 262, 627
- Lacey, C., & Cole, S. 1994, *MNRAS*, 271, 676
- Lee, J., & Shandarin, S. F. 1998, *ApJ*, 500, 14
- Lee, J. 2006, *ArXiv Astrophysics e-prints*, arXiv:astro-ph/0605697
- Lemson, G., & Kauffmann, G. 1999, *MNRAS*, 302, 111
- Mo, H. J., Yang, X., van den Bosch, F. C., & Katz, N. 2005, *MNRAS*, 363, 1155
- Mo, H. J., & White, S. D. M. 1996, *MNRAS*, 282, 347

- Percival, W. J., Scott, D., Peacock, J. A., & Dunlop, J. S. 2003, MNRAS, 338, L31
- Porciani, C., Catelan, P., & Lacey, C. 1999, ApJ, 513, L99
- Press, W. H., & Schechter, P. 1974, ApJ, 187, 425
- Sasaki, S. 1994, PASJ, 46, 427
- Sheth, R. K., Mo, H. J., & Tormen, G. 2001, MNRAS, 323, 1
- Sheth, R. K., & Lemson, G. 1999, MNRAS, 304, 767
- Sheth, R. K., & Tormen, G. 1999, MNRAS, 308, 119
- Taruya, A. & Suto, Y. 2000, ApJ, 542, 559
- Wang, H.Y., Mo, H.J., Jing, Y.P. 2006, ArXiv Astrophysics e-prints, arXiv:astro-ph/0608690
- Wechsler, R. H., Bullock, J. S., Primack, J. R., Kravtsov, A. V., & Dekel, A. 2002, ApJ, 568, 52
- Wechsler, R. H., Zentner, A. R., Bullock, J. S., & Kravtsov, A. V. 2005, ArXiv Astrophysics e-prints, arXiv:astro-ph/0512416
- Wetzel, A. R., Cohn, J. D., White, M., Holz, D. E., & Warren, M. S. 2006, ArXiv Astrophysics e-prints, arXiv:astro-ph/0606699
- Yang, X., Mo, H. J., & van den Bosch, F. C. 2006, ApJ, 638, L55
- Yoshikawa, K., Jing, Y.P., Taruya, A., & Suto, Y. 2001, ApJ, 558, 520
- Zhao, D. H., Mo, H. J., Jing, Y. P., Börner, G. 2003a, MNRAS, 339, 12
- Zhao, D. H., Jing, Y. P., Mo, H. J., Börner, G. 2003b, ApJ, 597, L9
- Zhu, G., Zheng, Z., Lin, W. P., Jing, Y. P., Kang, X., & Gao, L. 2006, ApJ, 639, L5

Table 1. Simulation parameters

boxsize( $h^{-1}$ Mpc)	particles	realizations	$m_{\text{particle}}$
300	$1024^3$	1	$1.8 \times 10^9 h^{-1} M_{\odot}$
600	$1024^3$	1	$1.5 \times 10^{10} h^{-1} M_{\odot}$
1200	$1024^3$	1	$1.2 \times 10^{11} h^{-1} M_{\odot}$
1800	$1024^3$	4	$4.0 \times 10^{11} h^{-1} M_{\odot}$

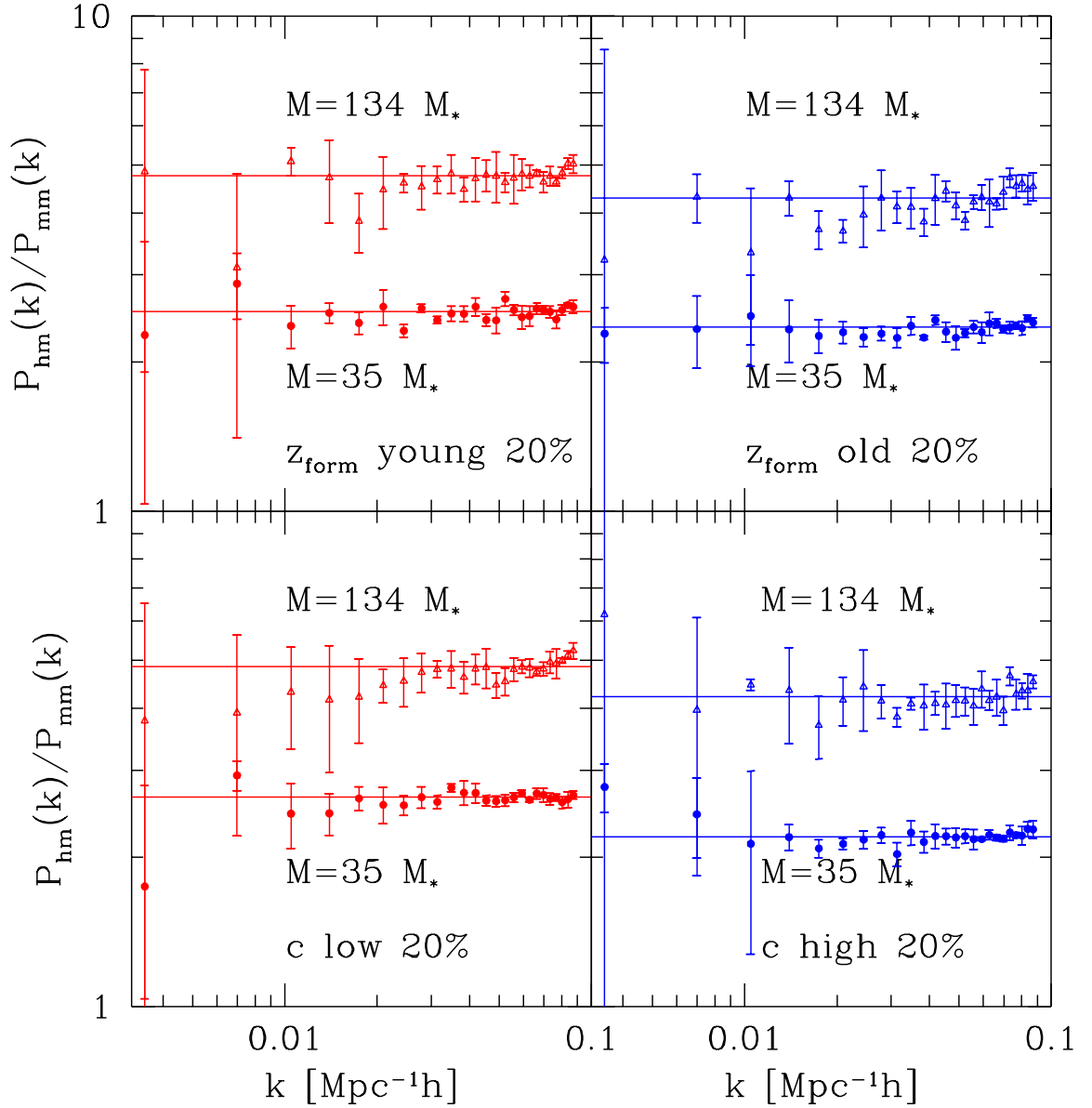


Fig. 1.— The ratio of the cross power spectrum  $P_{hm}(k)$  of halos with background dark matter to the matter power spectrum  $P_{mm}(k)$  versus the wavelength in the linear regime. The top left and right panels are for the 20% youngest and 20% oldest halos respectively, where the age is defined as the formation redshift  $z_f$ . The bottom left and right panels show the results for the 20% halos that have the highest and lowest concentrations respectively. The mass of the halos, in unit of the characteristic mass, is given in the panels.

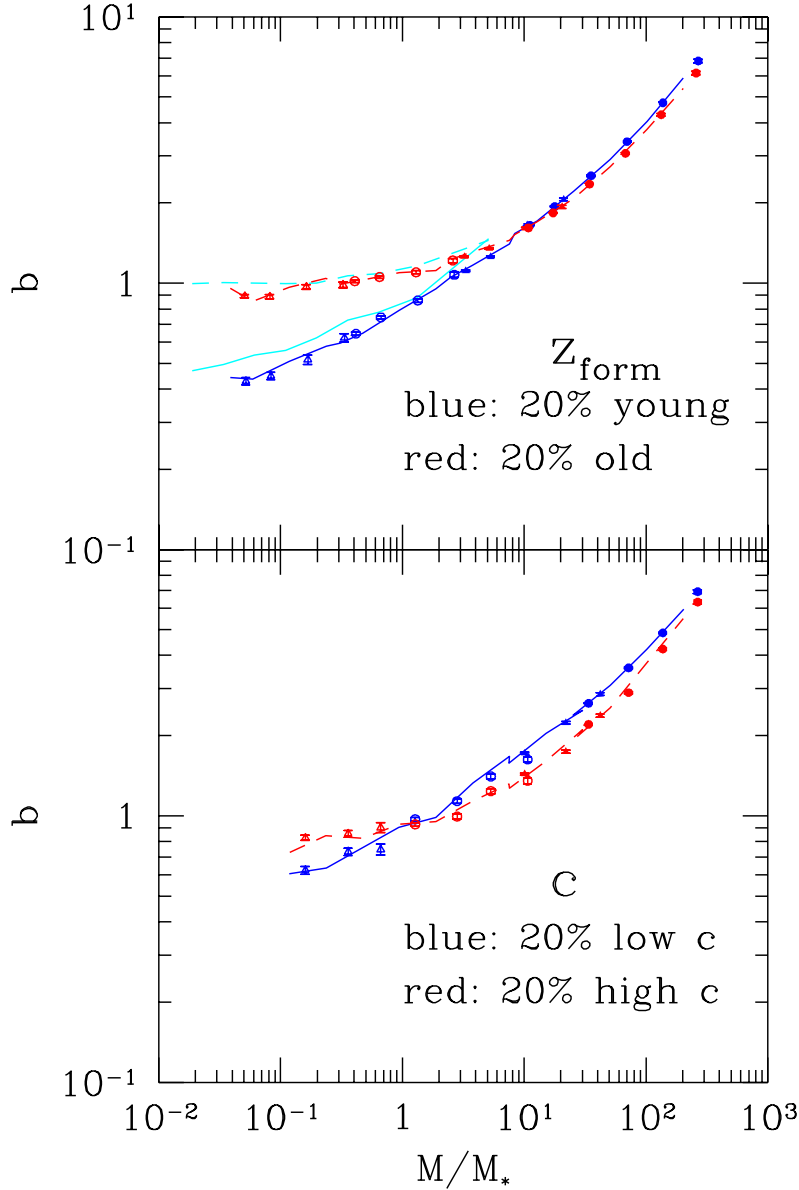


Fig. 2.— The bias factor of dark matter halos as a function of the halo mass. In the upper panel, we show the dependence on the halo formation epoch, with the symbols in red being for the 20% oldest halos and those in blue being for 20% youngest halos. The cyan lines are the results of Gao et al. (2005) for comparison. The lower panel shows the dependence on the halo concentration, with the red and blue colors being for those with the 20% highest and lowest concentrations respectively. The open triangles, open circles, filled triangles, and filled circles are from the simulations of boxsize  $300 h^{-1}\text{Mpc}$ ,  $600 h^{-1}\text{Mpc}$ ,  $1200 h^{-1}\text{Mpc}$  and  $1800 h^{-1}\text{Mpc}$  respectively. The solid and dashed lines are not the lines connecting the data points, but are for the results of young (or less concentrated) and old (or more concentrated) halos respectively estimated for a very narrow mass bin  $M \pm 0.1M$ .